Clinical Imaging 56 (2019) 63–68

Contents lists available at ScienceDirect

Clinical Imaging

journal homepage: www.elsevier.com/locate/clinimag

Cardiothoracic Imaging

Peripheral vessel and air bronchograms for detecting the pathologic patterns of subsolid nodules

Chenguang Zhang[a,1], Jianke Li[b,1], Mengyue Sun[a], Shujing Li[a,*], Jingyu Li[a], Quanhai Li[c], Zhenlong Zhu[d]

[a] Department of Radiology, the First Hospital of Hebei Medical University, Shijiazhuang 050031, Hebei, China
[b] Department of Thoracic Surgery, the First Hospital of Hebei Medical University, Shijiazhuang 050031, Hebei, China
[c] Department of Cell Therapy Laboratory, the First Hospital of Hebei Medical University, Shijiazhuang 050031, Hebei, China
[d] Department of Pathology, the First Hospital of Hebei Medical University, Shijiazhuang 050031, Hebei, China

ARTICLE INFO

Keywords:
Subsolid nodule
Air bronchogram
Vessel
Lung adenocarcinoma
Pathology
Computed tomography

ABSTRACT

Purpose: To assess the relationships of subsolid nodules (SSNs) with peripheral vessels and aerated bronchi using computed tomography (CT), and to correlate the imaging features with the benign/malignant pathological diagnoses.

Methods: This study retrospectively analyzed data from 83 patients with a solitary SSN (January 2008 to December 2016). SSNs were imaged (LightSpeed 64-slice spiral CT, General Electric, USA), their mean diameter determined, and the relationship with peripheral vessels (types I-IV) and aerated bronchi (types I-V) were classified. Pathologic diagnoses were obtained from the surgical specimens.

Results: SSNs were diagnosed as benign (n = 29), pre-invasive (n = 9), micro-invasive adenocarcinoma (n = 7) and invasive adenocarcinoma (n = 38). SSN size, peripheral vessel class and aerated bronchus class differed between pathologic types ($P < 0.05$). For benign SSNs, peripheral vessel type II (58.6%) was most common, followed by III (20.7%) and IV (6.9%). Aerated bronchus type V (65.5%) was most frequent, followed by IV (27.6%); type I aerated bronchus was not observed. No cases of micro-invasive or invasive adenocarcinoma were peripheral vessel type I or aerated bronchus type V. For invasive adenocarcinoma, 92.1% were peripheral vessel types III + IV while 71.8% were aerated bronchus types I + II.

Conclusions: SSN pathologic types differ with regard to peripheral vessel and aerated bronchus types. Type I peripheral vessel and type V aerated bronchus (both least involved) suggest a benign lesion, whereas type III/IV peripheral vessel and type I/II aerated bronchus (both most involved) suggest malignancy.

1. Introduction

Lung cancer is currently the malignancy with the highest mortality worldwide [1]. Lung cancer comprises various pathologic types with different etiologies and is generally classified into small-cell lung cancer (SCLC) and non-small-cell lung cancer (NSCLC) [2,3]. NSCLC in turn encompasses three major groups according to the tumor cell type: adenocarcinoma, squamous cell carcinoma and large cell carcinoma [4,5]. Adenocarcinoma is the main pathologic class of lung cancer and its incidence has steadily increased [6]. Lung adenocarcinoma can manifest as solid nodules (SNs) or as subsolid nodules (SSNs) [7,8] observed by computed tomography (CT). Pulmonary SSNs appear as pure ground-glass nodules (GGNs) or part-solid GGNs and show a high rate of detection by pulmonary CT [9]. Although the incidence of SSNs is lower than that of SNs, the likelihood of malignancy is greater in SSNs [10,11]. The main pathologic types of pulmonary SSNs, especially persistent ones, are adenocarcinoma, precancerous lesions [9] and benign lesions resulting from (for example) infection, organized pneumonia, focal fibrosis, inflammation and bleeding [12].

Air bronchoscopic classification can predict the invasion of small lung adenocarcinoma, with obstruction, distortion or dilation of the bronchus, particularly in the solid part of a SSN, indicating a higher probability of malignancy [13]. Similarly, the GGN-vessel classification can help to distinguish benign from malignant lesions [14]; this is because tumor growth is critically dependent on blood supply, and malignant lesions are often associated with vascular changes such as

* Corresponding author.
E-mail address: lishujing1976@126.com (S. Li).
[1] These authors contributed equally to this work.

https://doi.org/10.1016/j.clinimag.2019.03.010
Received 9 February 2018; Received in revised form 14 March 2019; Accepted 20 March 2019
0899-7071/ © 2019 Elsevier Inc. All rights reserved.

increased blood supply and clustering of blood vessels. Currently, the main treatment option for lung cancer is a comprehensive package based on surgery, and prognosis is closely associated with disease stage. Indeed, early diagnosis and treatment is critical for improving survival in patients with lung cancer [15–17]. Prognosis could be improved if SSNs found by CT were accurately characterized to allow appropriate intervention. Therefore, we hypothesized that the relationship of a SSN to bronchi and vessels, categorized by imaging features, can differentiate probably benign from probably malignant nodules.

2. Material and methods

2.1. Study participants

This retrospective study analyzed data from consecutive patients with solitary intrapulmonary SSNs identified by CT at our hospital between January 2008 and December 2016. The inclusion criteria were: (1) 30–80 years of age; (2) solitary intrapulmonary SSN detected by CT; and (3) pathologic diagnosis made by examination of a surgically resected specimen. The exclusion criteria were: (1) history of primary malignancy; (2) history of chronic lung disease; (3) history of asbestos exposure; (4) history of dust allergy; (5) history of drug allergy; or (6) diagnosis by surgical pathology not available. All the participants included in the analysis were treated and followed-up in accordance with the 2013 recommendations of the Fleischner Society for the management of SSNs detected by CT [18]. The study protocol was approved by the Ethics Committee of the local Hospital. The requirement for written informed consent from the participants was waived due to the retrospective and anonymized design of the study.

2.2. CT imaging

A LightSpeed 64-slice spiral CT (General Electric, Boston, MA, USA) was used for pulmonary imaging. The patients were placed in the supine position with two arms raised above head. Each participant was instructed to hold breath at the end of deep inspiration, and spiral CT scanning was undertaken from the thoracic inlet to the costophrenic angle. The scanning parameters were: voltage, 120 kV; current, 8 mA; pitch, 0.938; layer thickness, 5 mm; interval, 5 mm; matrix, 512 × 512; lung window width, 1500 HU; lung window level, −550 HU; mediastinum window width, 350 HU; mediastinum window level, 40 HU. The acquired data underwent high-resolution lung algorithm reconstruction with a layer thickness and interval of 1.25 mm each.

2.3. Analysis of CT data

The lesion size was measured in the lung window, in accordance with the methods described by the 2017 recommendations of the Fleischner Society [19] and was quantified as the mean diameter, *i.e.* the sum of the largest and smallest diameters divided by two [20]. The lesions were divided into three groups based on size: diameter ≤ 1.0 cm, 1.0 cm < diameter < 2.0 cm, and diameter ≥ 2.0 cm [21].

The relationship between the pulmonary SSN and peripheral blood vessels (both arteries and veins) was classified into four types [14]: type I, peripheral blood vessels bypassed the SSN; type II, peripheral blood vessels passed through the SSN without distortion or distension; type III, distorted and distended peripheral blood vessels passed through the SSN; and type IV, more complex peripheral vasculature pattern than that listed above.

The relationship between the pulmonary SSN and the aerated bronchi was classified into five types, based on a previous study [22] and with small modifications: type I, the bronchus was obstructed abruptly by the solid component of the SSN; type II, the bronchus penetrated into the solid component of the SSN, with or without distortion and distension; type III, the bronchus penetrated into the ground-glass component of the SSN, with distortion and dilation, but did not penetrate into the solid component of the SSN; type IV, the bronchus penetrated into the ground-glass component of the SSN without distortion or dilation; and type V, the bronchus bypassed the SSN.

Three radiologists (with 5 years, 14 years and 17 years of experience in thoracic radiology, respectively) performed the evaluations. Analysis of the images for each patient was carried out independently by two of the three thoracic radiologists, who were blinded to the pathologic results. If discordance occurred, consensus was reached after mutual discussion or consultation with a third senior radiologist.

2.4. Pathologic diagnosis

Surgically resected specimens were collected and examined histologically using hematoxylin/eosin staining and immunohistochemistry. Two senior pathologists (with substantial experience in the histologic diagnosis of pulmonary lesions) made all the pathologic diagnoses, and (if necessary) consensus was reached by discussion.

The pathologic diagnosis was made using the 2011 International Association for the Study of Lung Cancer (IASLC)/American Thoracic Society (ATS)/European Respiratory Society (ERS) classification criteria and the 2015 World Health Organization classification of tumors (which follows the IASLC/ATS/ERS 2011 criteria with only minor changes) [23,24]. This classification of lung adenocarcinoma uses subtypes such as adenocarcinoma *in situ*, wall-growth-based adenocarcinoma and mucinous adenocarcinoma to replace bronchioloalveolar carcinoma in previous classifications. The classification also defines micro-invasive adenocarcinoma as a subtype, abolishing mixed lung adenocarcinoma, and classifies atypical adenomatous hyperplasia and adenocarcinoma *in situ* as pre-invasive lesions [23]. In the present study, pre-invasive lesions, micro-invasive adenocarcinomas and invasive adenocarcinomas were classified as malignant nodules [23,24].

2.5. Statistical analysis

SPSS19.0 software (IBM Corp., Armonk, NY, USA) was used for the statistical analyses. Categorical variables are expressed as n (%) and were compared using Pearson's χ^2 test or Fisher's exact test when appropriate. Continuous data are expressed as the mean ± standard deviation and were compared using the Student t-test. $P < 0.05$ was considered statistically significant.

3. Results

3.1. Baseline clinical characteristics of the study participants

A total of 83 patients were enrolled, including 31 males and 52 females, aged 39–78 years (mean age, 57.75 ± 9.04 years). There were 2 cases with chest pain, 10 with cough, 8 with sputum, 2 with bloody sputum, and 71 without symptoms. The surgical pathology diagnoses were: 7 cases of adenocarcinoma *in situ*, 2 cases of atypical adenomatous hyperplasia, 7 cases of micro-invasive adenocarcinoma, 11 cases of well-differentiated invasive adenocarcinoma, 27 cases of moderately differentiated invasive adenocarcinoma, and 29 cases of benign nodules. No metastases were found. The clinical characteristics of the 83 participants are shown in Table 1. Representative CT images are shown in Figs. 1–4.

3.2. Associations of SSN pathologic type with lesion size

A significant association between pathologic pattern and lesion size was also observed ($\chi^2 = 104.35$, $P < 0.001$; Table 2). Lesion size in the pre-invasive adenocarcinoma group was significantly larger than that in the benign ($P < 0.01$) and micro-invasive adenocarcinoma ($P < 0.05$) groups. SSN diameter in the invasive adenocarcinoma group was significantly larger than that in the benign, pre-invasive

Table 1
Patient baseline data.

	Benign (n = 46)	Malignant (n = 42)	*P* value
Gender (male)	16(34.8%)	19 (45.2%)	0.317
Age	59.3 ± 9.2(39–78)	56.9 ± 8.3 (41–75)	0.197
Clinical symptoms (yes)	5 (10.9%)	5 (11.9%)	0.879
Basic disease (yes)	7 (15.2%)	6 (14.3%)	0.902
Diabetes	4 (8.7%)	3 (7.1%)	0.788
Hypertension	3 (6.5%)	2 (4.8%)	0.722
tympanitis	0 (0%)	1 (2.4%)	0.477

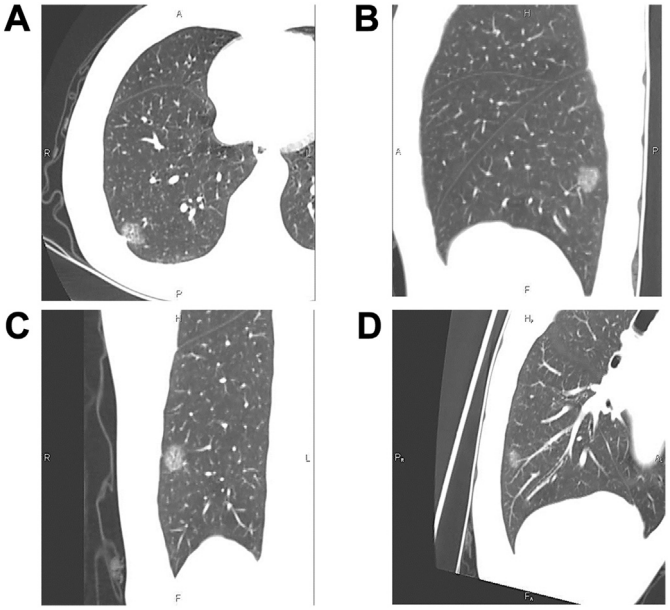

Fig. 1. Representative CT images from a 65-year-old female. The lower lobe of the right lung contained a subsolid nodule of mean diameter 1.6 cm. A: Axial plane. B: Coronal plane. C: Sagittal plane. D: Curved planar reformation. The lesion was classified as peripheral blood vessel class II and aerated bronchus class IV. The pathologic pattern was that of smooth muscle hyperplasia.

adenocarcinoma and micro-invasive adenocarcinoma groups (all $P < 0.001$).

3.3. Association of SSN pathologic type with peripheral blood vessel classification

There was a significant association between peripheral blood vessel classification and pathologic pattern ($\chi^2 = 77.82$, $P < 0.001$; Table 2). Notably, peripheral blood vessel class was significantly higher (types III-IV, greatest vessel involvement) in the invasive adenocarcinoma group than in the benign, pre-invasive adenocarcinoma and micro-invasive adenocarcinoma groups (all $P < 0.001$).

3.4. Association of SSN pathologic type with aerated bronchus classification

Comparisons of the aerated bronchus classifications between the various pathologic subtypes revealed statistically significant differences between all the pathologic groups ($\chi^2 = 257.36$, $P < 0.001$). Aerated bronchus class was significantly lower (classes I-II, aerated bronchi involved with the SSN) in all three malignant groups than in the benign lesion group (all $P < 0.001$). Aerated bronchus class was also lower (classes I-II, aerated bronchi involved with the SSN) in the micro-invasive adenocarcinoma and invasive adenocarcinoma groups than in the pre-invasive group ($P < 0.05$ and $P < 0.001$, respectively), as well as in the invasive adenocarcinoma group compared with the micro-invasive adenocarcinoma group ($P < 0.001$) (Table 2).

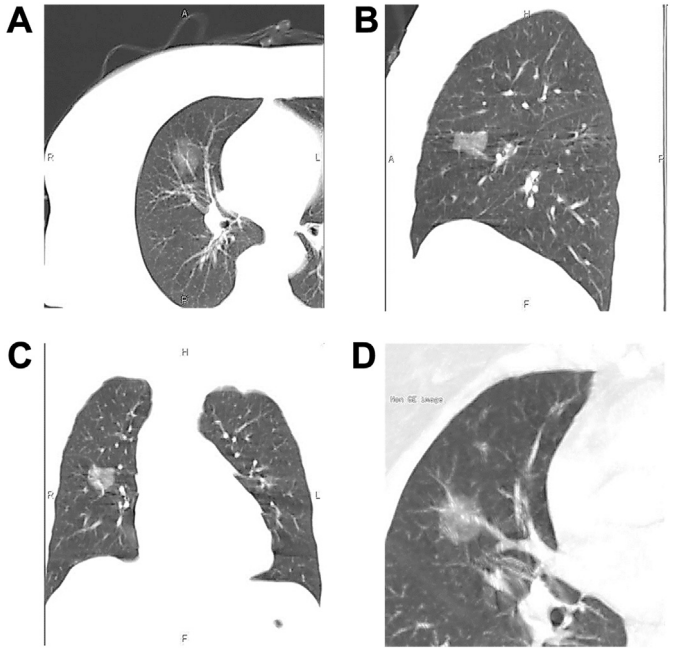

Fig. 2. Representative CT images from a 67-year-old female. The middle lobe of the right lung contained a subsolid nodule of mean diameter 2.5 cm. A: Axial plane. B: Sagittal plane. C: Coronal plane. D: Curved planar reformation. The lesion was classified as peripheral blood vessel class III and aerated bronchus class II. The pathologic pattern was that of an invasive adenocarcinoma.

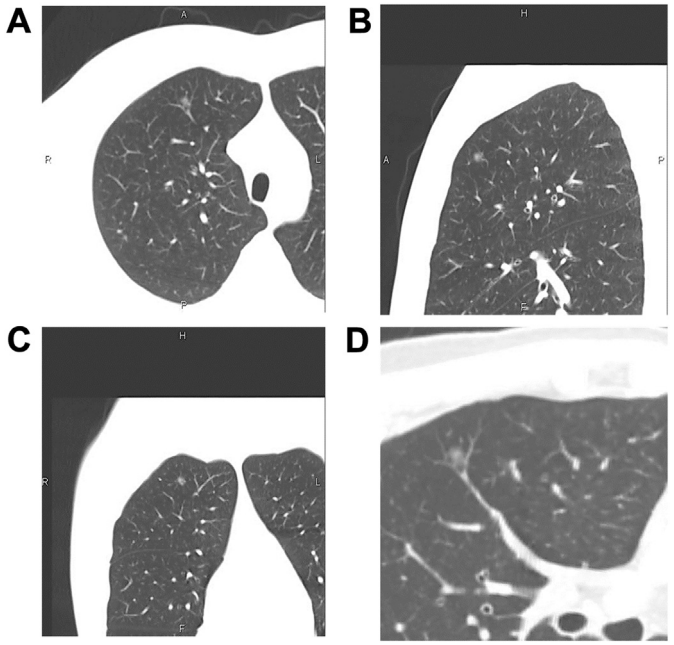

Fig. 3. Representative CT images from a 41-year-old male. The upper lobe of the right lung contained a pure ground-glass nodule of mean diameter 0.7 cm. A: Axial plane. B: Sagittal plane. C: Coronal plane. D: Curved planar reformation. The lesion was classified as peripheral blood vessel class II and aerated bronchus class III. The pathologic pattern was that of an pre-invasive adenocarcinoma.

4. Discussion

This study strongly suggests that the various pathologic types of SSN exhibit significant differences with regard to the peripheral blood vessel class and aerated bronchus class determined from CT images. In

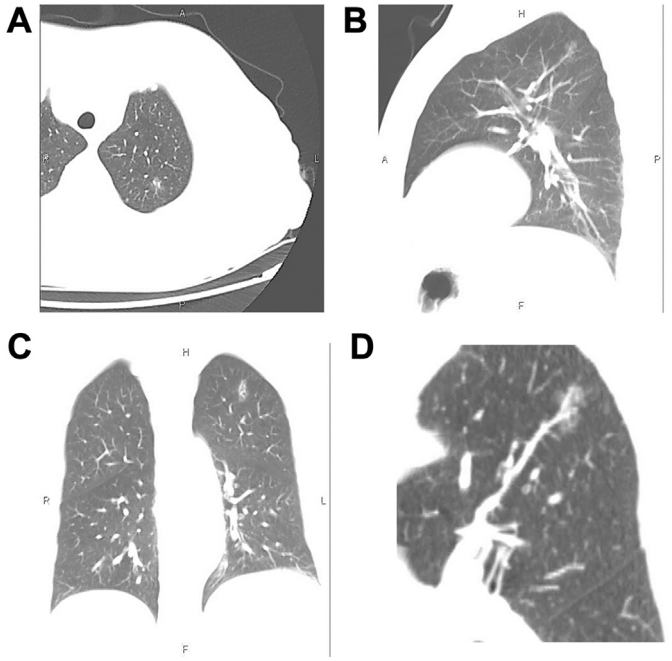

Fig. 4. Representative CT images from a 67-year-old female. The upper lobe of the left lung contained a subsolid nodule of mean diameter 1.4 cm. A: Axial plane. B: Sagittal plane. C: Coronal plane. D: Curved planar reformation. The lesion was classified as peripheral blood vessel class III and aerated bronchus class III. The pathologic pattern was that of an pre-invasive adenocarcinoma.

particular, peripheral blood vessel type I (least involved) and aerated bronchus type V (least involved) tended to indicate a benign lesion, while peripheral blood vessel types III/IV (most involved) and aerated bronchus types I/II (most involved) tended to reflect malignancy.

Our data clearly suggest that peripheral blood vessel type I was associated with a high likelihood of a benign tumor, while type III or type IV (most involved) suggested a high possibility of malignancy. However, peripheral blood vessel type II was commonly found for both benign and malignant lesions. The observed association between peripheral blood vessel classification and tumor pathologic type likely reflects the importance of blood supply to the growth of a malignant tumor. During the early stages, tumor cells obtain nutrients mainly through capillaries dispersed within the tissue. However, when tumors reach a size of 1–2 mm, growth becomes difficult without additional blood supply routes [25]. Currently described additional blood supply routes to lung cancer include angiogenesis and vasculogenic mimicry (VM) [26]. It is well known that tumor neovascularization leads to diverse vascular morphologies and inhomogeneous blood vessel diameter. On CT analysis, peripheral blood vessel types III and IV (most involved) are mainly characterized by increased vessel branching as well as vessel distortion and distension. As described above, among the 28 cases with a type II (less involved) relationship between the SSN and blood vessels, there were 17 with benign nodules, 4 with precancerous lesions, 4 with micro-invasive adenocarcinoma and 3 with invasive adenocarcinoma. A possible reason for why a type II SSN-blood vessel relationship (less involved) is often observed for both benign and malignant lesions is that the blood supply of an invasive adenocarcinoma might originate from VM, with no visible neovascularization. Therefore, many adenocarcinomas exhibit no morphologic changes in the peripheral vessels on CT [27,28]. Gao et al. [14] believed that the spatial relationships between GGNs and supplying blood vessels could be categorized into four types: I, vessels passing by GGNs; II, intact vessels passing through GGNs; III, distorted, dilated or tortuous vessels seen within GGNs; IV, more complicated vasculature other than described above. Tumor growth requires blood supply. The richer the blood supply, the stronger the basis for supporting its growth. The possibility of malignancy is very small when there is no additional or abundant blood supply. Hence, in the presence of type I, the likelihood of the SSN being malignant is low, while type IV suggested abundant and abnormal blood supply. The present study adds to the literature by providing additional benign cases to confirm their association with class I blood supply.

Among the 29 cases with benign nodules in the present study, 8 were type IV (less involved) and 19 were type V (least involved) with regard to the aerated bronchus classification. By contrast, type I was most common in the 38 cases with invasive adenocarcinoma,

Table 2
Associations between SSN pathologic type with types of aerated bronchus, types of peripheral vessel, location of lesions, and size of lesions.

	Benign lesions	Pre-invasive lesions	Micro-invasive adenocarcinoma	Invasive adenocarcinoma	*P*
	(n = 29)	(n = 9)	(n = 7)	(n = 38)	
Types of aerated bronchus		*	*	*,&,#	< 0.001
I	0	1 (11.1)	2 (28.6)	21 (55.3)	
II	1 (3.4)	2 (22.2)	0	7 (18.4)	
III	1 (3.4)	4 (44.4)	5 (71.4)	1 (2.6)	
IV	8 (27.6)	1 (11.1)	0	9 (23.7)	
V	19 (65.5)	1 (11.1)	0	0	
Types of peripheral vessel				*,#	< 0.001
I	4 (13.8)	1 (11.1)	0	0	
II	17 (58.6)	4 (44.4)	4 (57.1)	3 (7.9)	
III	6 (20.7)	3 (33.3)	3 (42.9)	23 (60.5)	
IV	2 (6.9)	1 (11.1)	0	12 (31.5)	
Location					0.460
Left upper lobe	7 (24.1)	4 (44.4)	1 (14.3)	7 (18.4)	
Left inferior lobe	4 (13.8)	3 (33.3)	1 (14.3)	12 (31.6)	
Right upper lobe	8 (27.6)	2 (22.2)	4 (57.1)	12 (31.6)	
Right middle lobe	3 (10.3)	0	0	2 (5.3)	
Right inferior lobe	7 (24.1)	0	1 (0.0)	5 (13.2)	
Diameter				*,#	< 0.001
≤1.0 cm	23 (79.3)	3 (33.3)	5 (71.4)	4 (10.5)	
1.0–2.0 cm	5 (17.2)	6 (66.7)	2 (28.6)	21 (55.3)	
≥2.0 cm	1 (3.4)	0	0	13 (34.2)	

* $P < 0.008$ *vs.* benign lesions.
& $P < 0.008$ *vs.* precancerous lesions.
# $P < 0.008$ *vs.* micro-invasive adenocarcinoma.

accounting for 55.3% of cases. Type V (least involved) was not found in pre-invasive lesions, micro-invasive adenocarcinoma or invasive adenocarcinoma. Importantly, aerated bronchus type was the only parameter that differed significantly between every group, indicating that it may have the potential to distinguish between benign lesions, pre-invasive lesions, micro-invasive adenocarcinoma and invasive adenocarcinoma. Our findings suggest that a type V aerated bronchus (least involved) reflects a high possibility of a benign lesion, whereas types I and II suggest malignancy. However, a type III or IV aerated bronchus could indicate the presence of a benign or malignant lesion. Lung adenocarcinoma usually originates from the mucosal and glandular epithelia of the bronchus and can grow outside and/or inside the bronchus or along the bronchial wall, although adenocarcinoma tends to grow outside the bronchus. The various patterns of growth can lead to thickening of the bronchial wall, a tortuous course and local distension. When no bronchus is found in the lesion, lung adenocarcinoma cannot have developed pathologically, and hence the lesion is benign. Consistent with this proposal, all type V (least involved) nodules in the present study were benign.

Another notable finding of this study was that SSN size was associated with pathologic type (Table 2). Eguchi et al. performed a retrospective study of 101 cases with intrapulmonary GGN, including 47 cases of adenocarcinoma *in situ*, 30 cases of minimally invasive adenocarcinoma (MIA) and 24 cases of invasive lung adenocarcinoma, and found that lesion size in the MIA and invasive lung adenocarcinoma groups was significantly larger than that in the adenocarcinoma *in situ* group [29]. Lee et al. showed that in pure GGNs, lesion < 10 mm discriminated between pre-invasive (smaller lesions) and invasive lesions (larger lesions) [30]. Takahashi et al. showed that pure GGNs > 10 mm were indicative of future lesions growth, suggesting their malignant potential [20]. A large retrospective study of 811 patients showed that lesion < 2.0 cm indicated a non-invasive malignant lesion [31]. This study also postulates a correlative finding that total lesion size ≥ 2 cm is indicative of malignancy.

The limitations of this study should be noted. First, this was a retrospective study, so it cannot be excluded that selection bias or reporting bias influenced our results. Second, this was a single-center study so the results may not be generalizable to the general patient population in China or elsewhere. Third, the number of cases included was small, which limits the strength of the conclusions that can be drawn. Fourth, receiver operating characteristic curve analysis was not performed to calculate the sensitivity and specificity of the CT-based classification systems for distinguishing benign from malignant lesions. Fifth, the repeatability of the CT analysis was not formally assessed through measurements of intra-observer and inter-observer variability, and the possible influence of a formal training program on measurement variability was not determined. Therefore, larger sample, well designed, prospective, multicenter studies are needed to confirm our findings.

5. Conclusion

In conclusion, CT-classified peripheral blood vessel involvement and aerated bronchus involvement may have potential for distinguishing malignant SSNs from benign lesions. Indeed, type I peripheral blood vessel class or type V aerated bronchus class (both least involved) is suggestive of a benign lesion, whereas type III/IV peripheral blood vessel class or type I/II aerated bronchus class (both most involved) is suggestive of malignancy. Further research is needed to establish whether these CT-based classifications could be used to assist in the diagnosis of SSNs and facilitate decision-making regarding treatment.

Acknowledgements

None.

Conflicts of interest

The authors declare that they have no conflict of interest.

Funding

This study was funded by Health Commission of Hebei Province, China (Grant number: 20160685).

References

[1] Siegel R, Naishadham D, Jemal A. Cancer statistics, 2013. CA Cancer J Clin 2013;63:2013.
[2] Wei MM, Zhou GB. Long non-coding RNAs and their roles in non-small-cell lung cancer. Genomics Proteomics Bioinformatics 2016;14:2016.
[3] Kodaz H, Tastekin E, Erdogan B, Hacibekiroglu I, Tozkir H, Gurkan H, et al. KRAS mutation in small cell lung carcinoma and extrapulmonary small cell cancer. Balkan Med J 2016;33:2016.
[4] Yano M, Yoshida J, Koike T, Kameyama K, Shimamoto A, Nishio W, et al. The outcomes of a limited resection for non-small cell lung cancer based on differences in pathology. World J Surg 2016;40:2016.
[5] Konopka KE. Diagnostic pathology of lung cancer. Semin Respir Crit Care Med 2016;37:2016.
[6] de Groot P, Munden RF. Lung cancer epidemiology, risk factors, and prevention. Radiol Clin North Am 2012;50:2012.
[7] Aoki T, Tomoda Y, Watanabe H, Nakata H, Kasai T, Hashimoto H, et al. Peripheral lung adenocarcinoma: correlation of thin-section CT findings with histologic prognostic factors and survival. Radiology 2001;220:2001.
[8] Godoy MC, Naidich DP. Subsolid pulmonary nodules and the spectrum of peripheral adenocarcinomas of the lung: recommended interim guidelines for assessment and management. Radiology 2009;253:2009.
[9] Kim H, Park CM, Koh JM, Lee SM, Goo JM. Pulmonary subsolid nodules: what radiologists need to know about the imaging features and management strategy. Diagn Interv Radiol 2014;20:2014.
[10] Henschke CI, Yankelevitz DF, Mirtcheva R, McGuinness G, McCauley D, Miettinen OS. CT screening for lung cancer: frequency and significance of part-solid and nonsolid nodules. AJR Am J Roentgenol 2002;178:2002.
[11] Jacobs C, van Rikxoort EM, Twellmann T, Scholten ET, de Jong PA, Kuhnigk JM, et al. Automatic detection of subsolid pulmonary nodules in thoracic computed tomography images. Med Image Anal 2014;2014(18).
[12] Seidelman JL, Myers JL, Quint LE. Incidental, subsolid pulmonary nodules at CT: etiology and management. Cancer Imaging 2013;13:2013.
[13] Zhang Y, Qiang JW, Shen Y, Ye JD, Zhang J, Zhu L. Using air bronchograms on multi-detector CT to predict the invasiveness of small lung adenocarcinoma. Eur J Radiol 2016;85:2016.
[14] Gao F, Li M, Ge X, Zheng X, Ren Q, Chen Y, et al. Multi-detector spiral CT study of the relationships between pulmonary ground-glass nodules and blood vessels. Eur Radiol 2013;23:2013.
[15] Asamura H, Hishida T, Suzuki K, Koike T, Nakamura K, Kusumoto M, et al. Radiographically determined noninvasive adenocarcinoma of the lung: survival outcomes of Japan Clinical Oncology Group 0201. J Thorac Cardiovasc Surg 2013;146:2013.
[16] Fukui T, Mitsudomi T. Small peripheral lung adenocarcinoma: clinicopathological features and surgical treatment. Surg Today 2010;40:2010.
[17] Tsutani Y, Miyata Y, Nakayama H, Okumura S, Adachi S, Yoshimura M, et al. Appropriate sublobar resection choice for ground glass opacity-dominant clinical stage IA lung adenocarcinoma: wedge resection or segmentectomy. Chest 2014;145:2014.
[18] Naidich DP, Bankier AA, MacMahon H, Schaefer-Prokop CM, Pistolesi M, Goo JM, et al. Recommendations for the management of subsolid pulmonary nodules detected at CT: a statement from the Fleischner Society. Radiology 2013;266:2013.
[19] MacMahon H, Naidich DP, Goo JM, Lee KS, Leung ANC, Mayo JR, et al. Guidelines for Management of Incidental Pulmonary Nodules Detected on CT Images: From the Fleischner Society 2017. Radiology 2017;284:2017.
[20] Takahashi S, Tanaka N, Okimoto T, Tanaka T, Ueda K, Matsumoto T, et al. Long term follow-up for small pure ground-glass nodules: implications of determining an optimum follow-up period and high-resolution CT findings to predict the growth of nodules. Jpn J Radiol 2012;30:2012.
[21] Shi CL, Zhang XY, Han BH, He WZ, Shen J, Chu TQ. A clinicopathological study of resected non-small cell lung cancers 2 cm or less in diameter: a prognostic assessment. Med Oncol 2011;28:2011.
[22] Wang Y, Liang KR, Liu XG, Wang JA, Kang JH, Liang MZ. Relationship between peripheral lung cancer and the surrounding bronchi, pulmonary arteries, pulmonary veins: a multidetector CT observation. Clin Imaging 2011;35:2011.
[23] Travis WD, Brambilla E, Noguchi M, Nicholson AG, Geisinger KR, Yatabe Y, et al. International association for the study of lung cancer/american thoracic society/european respiratory society international multidisciplinary classification of lung adenocarcinoma. J Thorac Oncol 2011;6:2011.
[24] Travis WD, Brambilla E, Nicholson AG, Yatabe Y, Austin JHM, Beasley MB, et al. The 2015 World Health Organization Classification of Lung Tumors: Impact of Genetic, Clinical and Radiologic Advances Since the 2004 Classification. J Thorac Oncol 2015;10:2015.

[25] Folkman J. Angiogenesis. Annu Rev Med 2006;57:2006.
[26] Jackson AL, Zhou B, Kim WY. HIF, hypoxia and the role of angiogenesis in non-small cell lung cancer. Expert Opin Ther Targets 2010;14:2010.
[27] Yao L, Zhang D, Zhao X, Sun B, Liu Y, Gu Q, et al. Dickkopf-1-promoted vasculogenic mimicry in non-small cell lung cancer is associated with EMT and development of a cancer stem-like cell phenotype. J Cell Mol Med 2016;20:2016.
[28] Wu S, Yu L, Cheng Z, Song W, Zhou L, Tao Y. Expression of maspin in non-small cell lung cancer and its relationship to vasculogenic mimicry. J Huazhong Univ Sci Technolog Med Sci 2012;32:2012.
[29] Tsutani Y, Miyata Y, Nakayama H, Okumura S, Adachi S, Yoshimura M, et al. Prognostic significance of using solid versus whole tumor size on high-resolution computed tomography for predicting pathologic malignant grade of tumors in clinical stage IA lung adenocarcinoma: a multicenter study. J Thorac Cardiovasc Surg 2012;143:2012.
[30] Lee HJ, Goo JM, Lee CH, Park CM, Kim KG, Park EA, et al. Predictive CT findings of malignancy in ground-glass nodules on thin-section chest CT: the effects on radiologist performance. Eur Radiol 2009;19:2009.
[31] Suzuki K, Koike T, Asakawa T, Kusumoto M, Asamura H, Nagai K, et al. A prospective radiological study of thin-section computed tomography to predict pathological noninvasiveness in peripheral clinical IA lung cancer (Japan Clinical Oncology Group 0201). J Thorac Oncol 2011;6:2011.